Paper Code: F02I112

INTEGRATED MULTI-BODY/FEM ANALYSIS OF VEHICLE DYNAMIC BEHAVIOUR

Biancolini, Marco Evangelos[1]*
Baudille, Riccardo[1]
Reccia, Luigi[1]

[1]Department of Mechanical Engineering "Tor Vergata" University, Rome Italy.

KEYWORDS
Kart, FEM, Multi-body, Dynamic Simulation, Tire

ABSTRACT
The chassis stiffness of a vehicle influences road dynamic behaviour. In a standard vehicle elastic behaviour is demanded to suspension elements; hence chassis has only the task to be tough and stiff enough to avoid elastic interaction with flexible parts. To satisfy the philosophy of simplicity, competition go-kart regulations require the absence of suspension systems and differential gear. Thus elastic frame characteristics are highlighted by the absence of suspension elements and the global dynamic behaviour is influenced by chassis shape and stiffness and by tires characteristics. Hence frame stiffness must be carefully evaluated in order to compensate the absence of differential gear by rising up the rear internal wheel during a turn. This avoids tire slip in favour of stability and acceleration and simultaneously assures a rigid connection between mechanical members. Moreover the development of tires performance has increased chassis importance whose shapes and materials have not substantial evolved. The reason is that tires development is practically the same of other formulas. Therefore kart tires can take advantage of a research results obtained elsewhere, on the contrary kart frames were developed only with knowledge of many years of experimentation and track tests. Nevertheless the great diffusion and popularity of karting sport, means great investments from corporations, privates and amateurs and karting is going to include a such high technological content to need design and analysis criterions peculiar to modern engineering.
The aim of this study is to develop and validate a numerical model which integrates FEM analysis with Multi-Body technique, in order to evaluate dynamic behaviour of a racing kart. The result is a useful tool in kart frame design. The FEM model was developed on the geometric model to evaluate the chassis stiffness. This model was validated by means of a static and dynamic loading tests. The static test consists of measuring displacements due to an application of a known load. This test is also useful to estimate a gross torsional stiffness value. Instead the dynamic response of the chassis, in order to check the FEM model dynamic capability, was measured by means of a load cell hammer/accelerometer system. Being the tires radial stiffness a very important parameter, because it ranges in values similar to the chassis stiffness and deeply influences load transfer in a kart, a set of experimental investigation was dedicated to properly evaluate this parameter.
The FEM analysis permits to estimate the kart frame displacements related to different load conditions (lateral and vertical force, flexural moment) applied to wheel hubs. The estimated stiffness is represented with an equivalent springs in an home-made Multi-Body model. The handling model was validated by results comparison with a commercial software.
The proposed procedure, based on the use of commercial software for FEM analysis and an home-developed code for Multi-Body, permits the optimisation of an existing kart frame and the new concept design.
A possible improvement of this procedure is the introduction of a shape optimisation algorithm that converge in a semiautomatic way to an optimal solution: structural parameters are varied to obtain a goal in dynamic simulation results, minimising, for instance, the lap time.

INTRODUCTION

In a standard vehicle design is assumed that the chassis has to be as stiff as possible, because the elastic behaviour is demanded to the suspension system. In fact one of the aims of the design is to optimise the chassis shape in order to obtain a prescribed stiffness [1]. A different approach is needed for those mechanical systems that don't have suspension elements. In this case the chassis is demanded to meet a particular elastic behaviour, thus the maximum stiffness criterion is not a good way to proceed. In these particular systems, called "compliant mechanisms" [2], the compliance of different parts of the frame is used to create mechanisms [3]. From this point of view, a competition go-kart could be reasonably considered as a compliant mechanism. In fact a kart is a very particular kind of vehicle: absence of suspension system and differential gear, driver and engine asymmetric position, special kind of braking system (it is allowed only on rear side in 100cc class) definitely increase chassis stiffness importance. Thus chassis has to satisfy very opposite requirements: a good match between braking (1), cornering (2) and accelerating (3) is needed. As shown in figure 1 is it possible to identify these three different phases around a single corner. For a good performance, in phase 1 high grip and stability is needed to have a fast deceleration; in phase 2 the deformation of the chassis has to lift up the rear internal tire, during the main part of a curve, avoiding the inevitable tire slip due to the absence of the differential gear; in phase 3 all tires firmly at the ground are required, in order to "free" the chassis and allow the maximum acceleration.

The design and setup of a competition go-kart were developed only with empirical methods. The result is a "natural evolution of the species": frame shapes we see today are only the individuals that survived to selection of many years of experimentation and track tests. Because of a great diffusion and popularity of karting sport, that means great investments from corporations, privates and amateurs, karting is going to posses a such technological content to need design and analysis criterions peculiar to modern engineering.

Every single element of the chassis influences global performance, so optimisation process may involve every component, according to ratification by international authority (CIK/FIA). There are two distinct sets of parameters to consider: the constructive ones and the set-up ones. Hence the tool proposed in this work is an analysis and design tool for first, but it could be a concrete help in set-up process too. For instance, more than the constructive structure, it is possible to work on toe, camber, caster, front/rear track width, wheel base, chassis height from the ground, rear axle stiffness, hubs kind and dimension, tire inflate pressure and driver position. About influence of drive position and its interaction with vehicle, two studies are reported on bibliography: the modelling of human body for movement analysis [4], and the development of a virtual dummy for the vibrational comfort analysis of car drivers [5]. Moreover is reported a previous work of the authors [6], that was used in [4] and introduce the present work. Dynamic effects connected with rolling pitching can easily handled [7], but are not accounted in the handling model proposed, because the interaction between the driver and the kart plays a crucial role considering that the drivers has about 50% of overall mass and is not rigidly connected to the kart. Further investigation are required to consider properly this interaction.

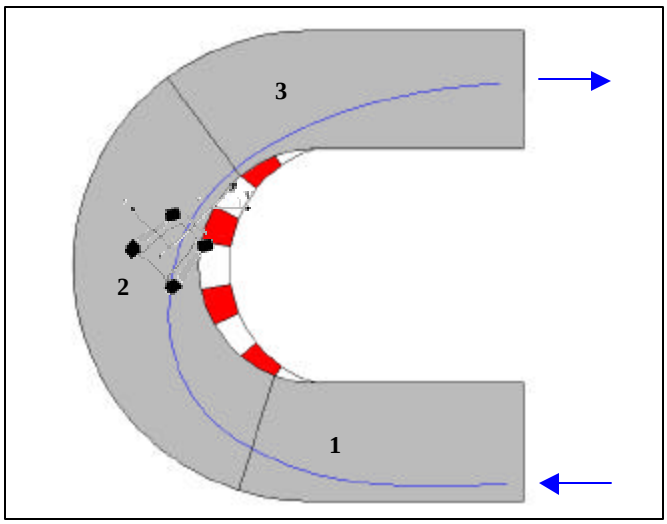

Figure 1: Three phases of a curve passing: 1 insertion; 2 cornering; 3 acceleration.

NUMERICAL MODEL

FEM model description

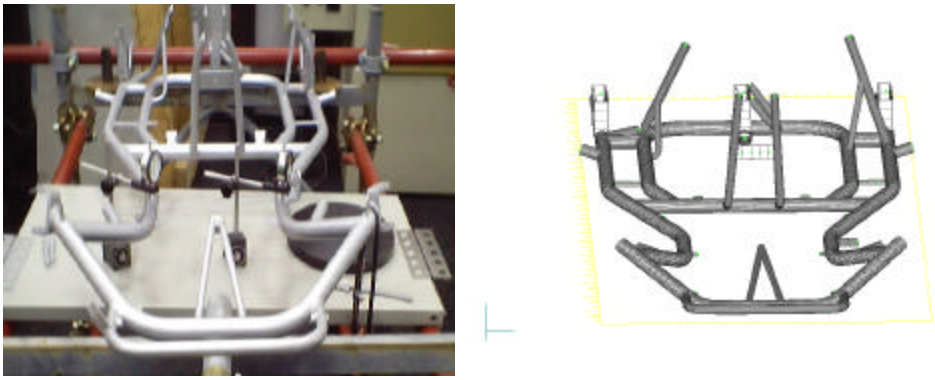

Figure 2: a) actual frame investigated; b) FEM model of the frame representing the actual cross section of BEAM elements.

The frame of the kart consists in a trellis build with various shaped cross sections, mainly of tubular type. The principal structure has a 32x2 circular tube section and consists in 12 bent and 12 straight parts and lies in an horizontal plane, with exception of the parts connected with stub axles that has a slight elevation. The other main elevation structures are the brackets interfacing seat, steering system and rear axle.
FEM model was prepared for the commercial solver MSC/Nastran V70.5 starting from the geometry of the middle line and is constituted of 561 CBEAM elements and 546 GRID points. A rendered representation is showed in Figure 2 in which the actual cross section of beam elements is illustrated.

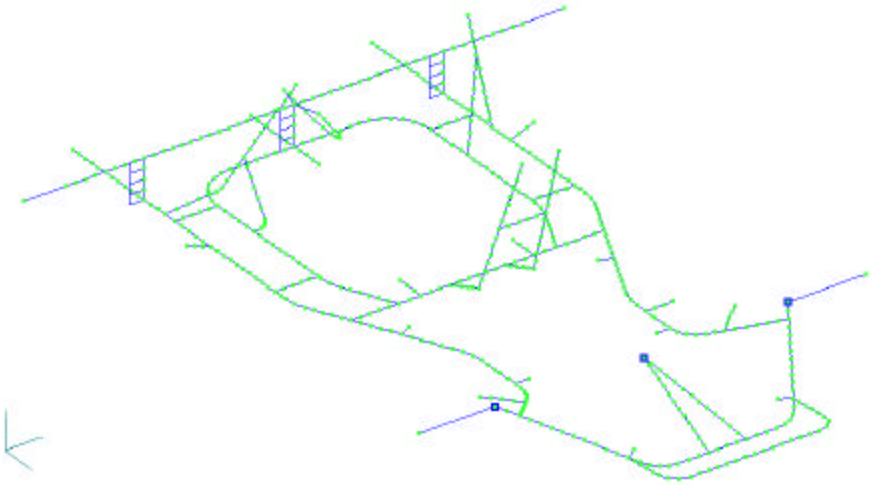

Figure 3:Complete FEM model used for the evaluation of frame stiffness.

The compliance of the frame was evaluated completing the FEM model with rear axle and connecting with rigid elements the middle point of each wheel, as illustrated in figure 3; this model allows to analyze the frame stiffness effects related to the displacements and rotation of wheel interfacing points. The last connection needed to properly evaluate elastic load transfer is with the vehicle center of mass. In this work overall mass was lumped in a rigid body connected to the frame in the interfacing points with seat, steering system and engine. Further investigations are required to model properly the actual mass distribution because the interaction vehicle-driver can produce important variation in the position of center of mass; the authors are already involved in the study of this interactions [4], and quantitative results will be presented in future works.

Handling Model

In order to simulate the dynamic behaviour of a kart during a generic road manoeuvre, a specific FORTRAN code has been written. The simulation model is based on equilibrium equations for the three degrees of freedom of a kart moving on a plane.

$$\begin{aligned} \sum F_x &= m\ddot{x} \\ \sum F_y &= m\ddot{y} \\ \sum M_z &= I\ddot{y} \end{aligned} \qquad (1)$$

Explicit integration of equations (1) permits to evaluate x, y and yaw acceleration basing on the longitudinal and lateral forces acting on the kart in the local co-ordinates system (see fig.4).

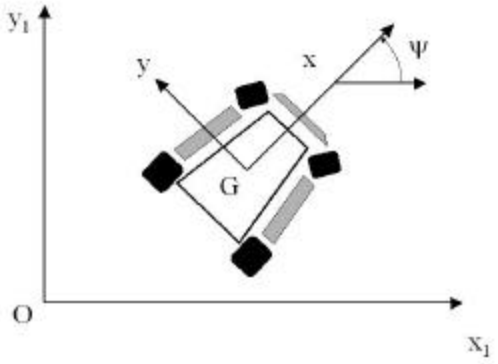

Figure 4: Frame reference adopted in dynamic analysis.

In this work aerodynamic actions are neglected, so only tire loads and weight appear in equilibrium equations. Although the handling model is planar, a simplified three-dimensional approach has been used to calculate vertical reaction on each tire. In fact, considering the kart chassis as a rigid body simply resting on four springs to the ground, is possible to solve the over-constrained (four bearings) three equations equilibrium problem (see fig. 5).

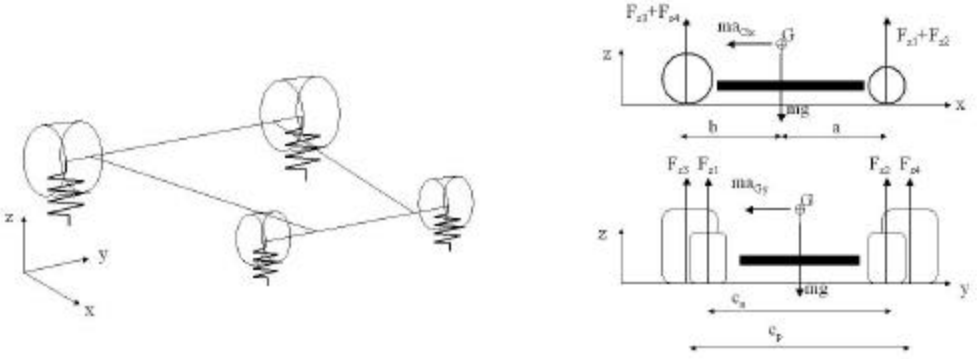

Figure 5: Elastic load transfer.

$$\begin{aligned} &F_{Z1} + F_{Z2} + F_{Z3} + F_{Z4} - mg = 0 \\ &(F_{Z3} + F_{Z4}) \cdot (a+b) - m\ddot{x} \cdot z_G - mga = 0 \\ &F_{Z2} \cdot c_a + F_{Z4} \cdot \left(\frac{c_a + c_p}{2} \right) - F_{Z3} \cdot \left(\frac{c_p - c_a}{2} \right) - mg \cdot \frac{c_a}{2} + m\ddot{y} \cdot z_G = 0 \end{aligned} \qquad (2)$$

In this model each of the four springs represents both tire and chassis stiffness. Chassis stiffness is evaluated using an algorithm of static condensation [6] based on the reduction of the FEM model to a limited degrees of freedom system. Applying this method to the vertical deformation of the point of the chassis corresponding to the wheel hubs, an order 4 matrix is obtained: hence the problem must be studied with a matricial approach.
Equations (2) can be written as

$$[A]\underline{F_z} + z_G \underline{b} = \underline{F_0} \tag{3}$$

where z_G variable is separated by F_Z variables. The wheel hubs displacements can be evaluated using linear rigid body approach (valid for little angles) disregarding inertial effect about rolling, pitch and vertical translation; this hypothesis, sometimes used in general vehicle modelling [8], seems much more justified for a suspensions-less vehicle. The equations are

$$\begin{aligned}
\Delta z_1 &= -z_G + j \cdot a + J.\frac{c_a}{2} + f_{11}(d) \\
\Delta z_2 &= -z_G + j \cdot a - J.\frac{c_a}{2} + f_{12}(d) \\
\Delta z_3 &= -z_G - j \cdot a + J.\frac{c_a}{2} \\
\Delta z_4 &= -z_G - j \cdot a - J.\frac{c_a}{2}
\end{aligned} \tag{4}$$

where z_G is the height of the centre of mass, j is the pitch angle and J is the rolling angle and f_1 represent the vertical movement of front tires during the steering, due to king-pin and caster angles. These equations can be expressed in matricial form with the following

$$\underline{\Delta z} = [E]\underline{q} + \underline{f_1} \tag{5}$$

where $q=(z_G, j, q)^T$. In this concentrated stiffness approach the wheel hubs sink can be divided into two terms due to tire and chassis stiffness:

$$\underline{\Delta z} = \underline{\Delta z}_T + \underline{\Delta z}_P = [C_T]\underline{F_Z} + [C_P]\underline{F_Z} \tag{6}$$

where $[C_T] = [K_T]^{-1}$ is the inverse of chassis stiffness matrix obtained with static condensation and

$$[C_P] = \begin{bmatrix} k_{PF} & 0 & 0 & 0 \\ 0 & k_{PF} & 0 & 0 \\ 0 & 0 & k_{PR} & 0 \\ 0 & 0 & 0 & k_{PR} \end{bmatrix}^{-1} \tag{7}$$

is a diagonal matrix, which contains radial stiffness of front (k_{PF}) and rear (k_{PR}) tires. Is possible to solve equation (6) in terms of $\underline{F_Z}$

$$\underline{\Delta z} = \left([C_T]\underline{F_Z} + [C_P]\right)\underline{F_Z} \Rightarrow \underline{F_Z} = \left([C_T]\underline{F_Z} + [C_P]\right)^{-1}\underline{\Delta z} = [K]\underline{\Delta z} \tag{8}$$

Substituting in (3)

$$[A][K]\underline{\Delta z} + z_G \underline{b} = \underline{F_0} \tag{9}$$

and considering (5)

$$[A][K]([E]\underline{q}+\underline{f_1})+z_G\underline{b}=\underline{F_0}$$
$$[A][K][E]\underline{q}+[A][K]\underline{f_1}+z_G\underline{b}=\underline{F_0} \qquad (10)$$
$$[D^*]\underline{q}+z_G\underline{b}=\underline{F_0}-[A][K]\underline{f_1}$$

where $[D^*]=[A][K][E]$, that is a system of three equations in $q=(z_G, j, J)^T$.
After obtaining $[D]$ merging $\underline{b}$ in $[D^*]$ the system solution is

$$\underline{q}=[D]^{-1}(\underline{F_0}-[A][K]\underline{f_1}) \qquad (11)$$

substituting (11) in (5) and then in (8) we have

$$\underline{F_z}=[K]([E]\underline{q}+\underline{f_1})=[K][E][D]^{-1}(\underline{F_0}-[A][K]\underline{f_1})+\underline{f_1}) \qquad (12)$$

that is the solution to the over-constrained problem in which vertical loads are expressed in terms of applied loads.
If one element of Dz is negative it means a tire have lost contact with the ground (that is favourable during a turn as described in the introduction): the equilibrium problem becomes isostatic and the solution is determined rearranging previous matrixes for three degrees of freedom.
Once vertical loads are determined for each tire, lateral forces can be evaluated using bi-linear model (see fig.6) which present a saturation when slip angle α and/or vertical load F_Z reach a fixed value. Values used for saturation are been determined basing on the knowledge of maximum value of lateral acceleration and using literature results [9].

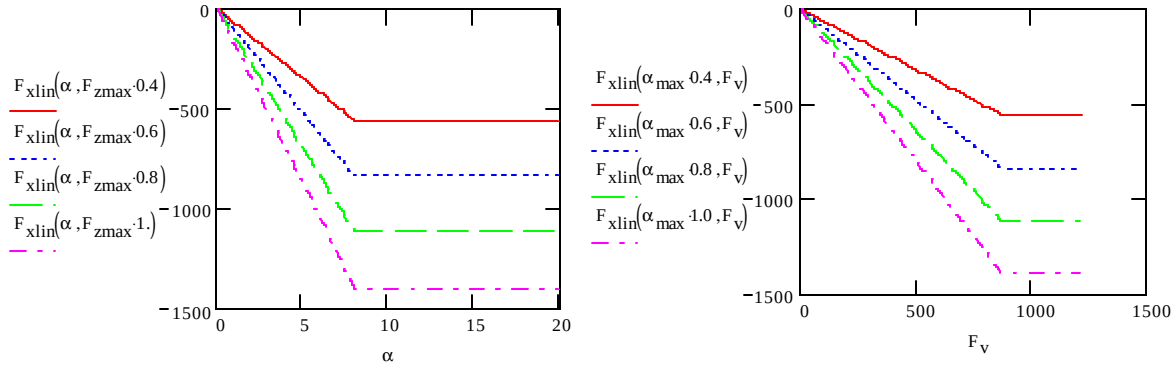

Figure 6: Linear model with saturation for the evaluation of later loads (N) in function of vertical load (N) and slip angle (deg).

Steering system

The geometry of the steering system influences kart dynamic in two ways. First, there is a relation between the rotation of the steering wheel and rotations of the front wheels governed by the quadrilateral cinematic: furthermore front wheels rotate around a raking axle defined by caster and king-pin angles; hence, during the steering, a change of the vertical position of the hub is observable. Both aspects have been introduced into the model. The quadrilateral cinematic has been studied as a planar mechanism using closure equation [10] (see fig. 7 and eq. 13)

$$AC\sin a + CD\cos b + DB\sin g = AB \qquad (13)$$

As shown in figure 7, the vertical movement of front tire's hubs has been evaluated analysing the spatial cinematic of a mobile coordinates system x"y"z' obtained rotating a coordinates system xyz (where x and y are the vehicle axis and z is orthogonal to the ground) of a king-pin angle (obtaining xy'z') and caster angle (obtaining x"y"z').

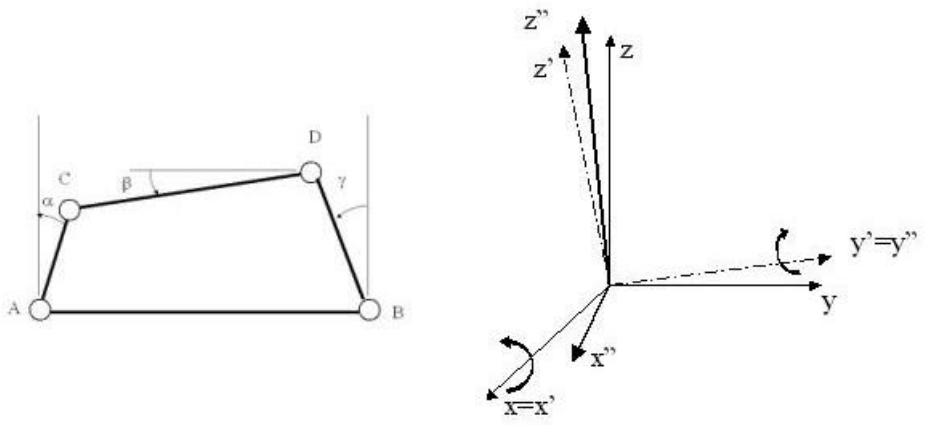

Figure 7: Steering system cinematic.

In this way is possible to calculate the vertical movement of the wheel hub acting a rotation of a steering angle around z" axis and using rotation matrix to obtain the new z position. Both quadrilateral and hub cinematic have been introduced into the model via representative equations. However a validation of the theoretical approach has been performed using a model of the steering system realised with a commercial multibody software, the Working Model 3D 5.0 (see figure 8).

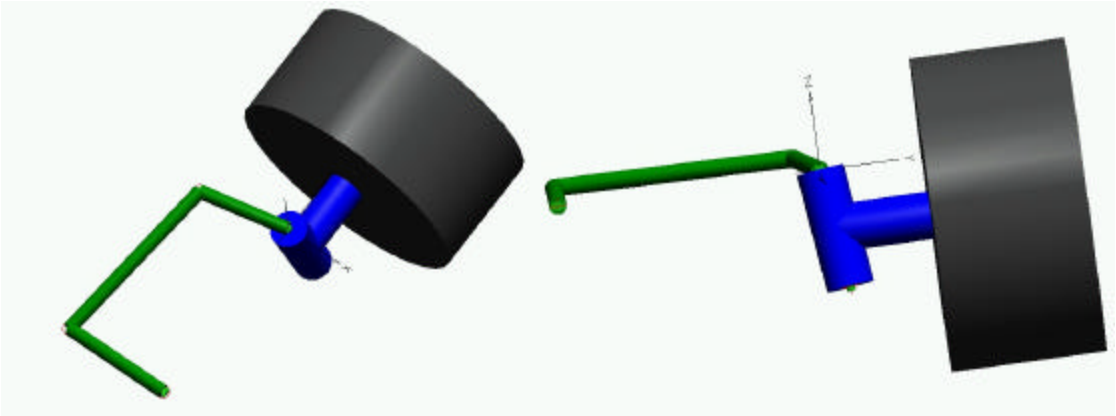

Figure 8: Steering system: multibody model.

Figure 9 shows the agreement between theoretical and Working Model simulation results in terms of vertical movement of the wheel hub versus steer angle

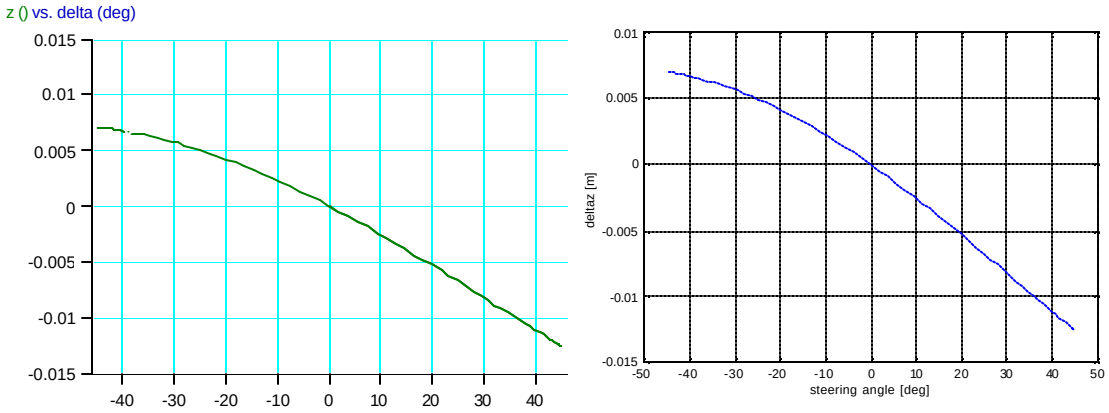

Figure 9: Comparison between proposed results and multibody code results.

EXPERIMENTAL

Tire radial stiffness

Radial stiffness of the tire is a very important parameter, especially for a kart, beacause has a deep influence in load transfer, being of the same order of the stiffness of the frame. Technical literature is poor of this data and a set of measurements was planned for the investigation of this parameter.

To achieve this aim was exploited an Universal Testing Machine Zwick equipped with a 5kN load cell. A suitable fixturing system was designed for the machine and is represented in fig. 10. The fixturing system consists in a very stiff support (segments A and B), connected to the base of the machine, that supports the actual axle (C), complete of bearing and interfaces to the wheel. Change of tire was quickly obtained because each tire tested was furnished with the complete wheel.

Of course, measured data include bearing and axle stiffness that for this reason are neglected in FEM model.

The fixturing system was completed by a compression platen: in this way the loading condition are nearly the same of road condition although the rolling effect is neglected. For this reason a corrective term, variable with vehicle speed, was inserted to account of the speed stiffening [11].

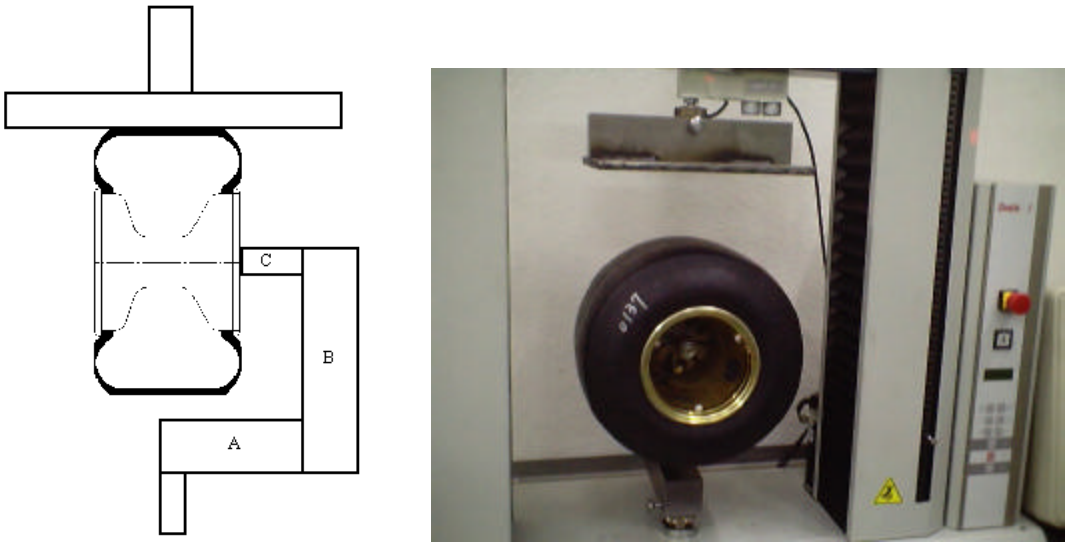

Figure 10: Radial stiffness testing layout.

Testing was conducted for six tires, a rear and front type of three different models (called in this paper Type1, Type2 and Type 3) at room temperature at four inflating pressure values (0.4bar, 0.6bar, 0.8bar, 1.0bar).

A typical recording, load-vs-displacement is reported in fig 11 for a front tire Type 1 inflated at the four pressure. We can observe a strong effect of inflating pressure, and an highly non linear behaviour at lower pressures.

Recorded curves show an initial region in which an increment in stiffness is observed due to the development of a complete footprint, followed by a linear region. To model the tire with a single stiffness parameter a last square linear regression was performed in the region 500N-1000N. In figures 12 are reported the results.

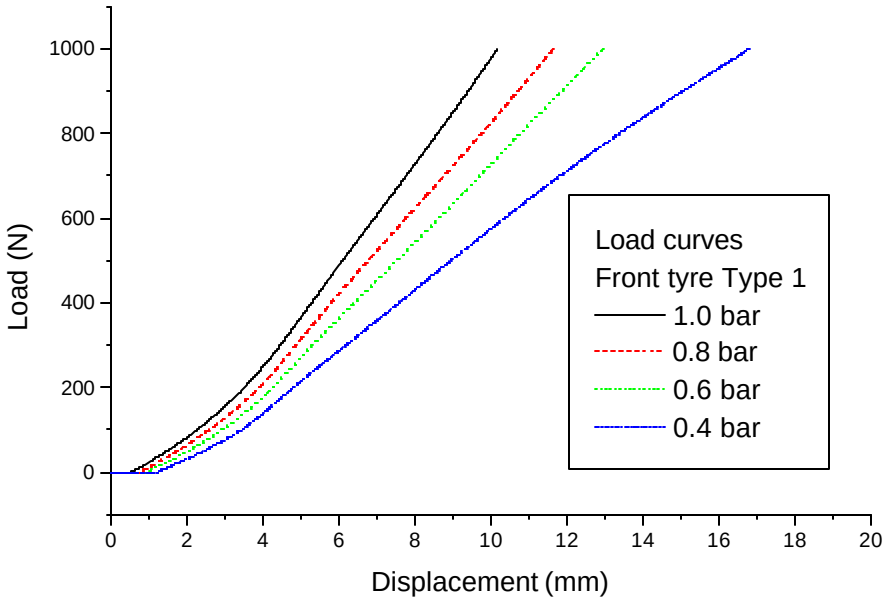

Figure 11: Load-displacements curves for a front tire Type 1.

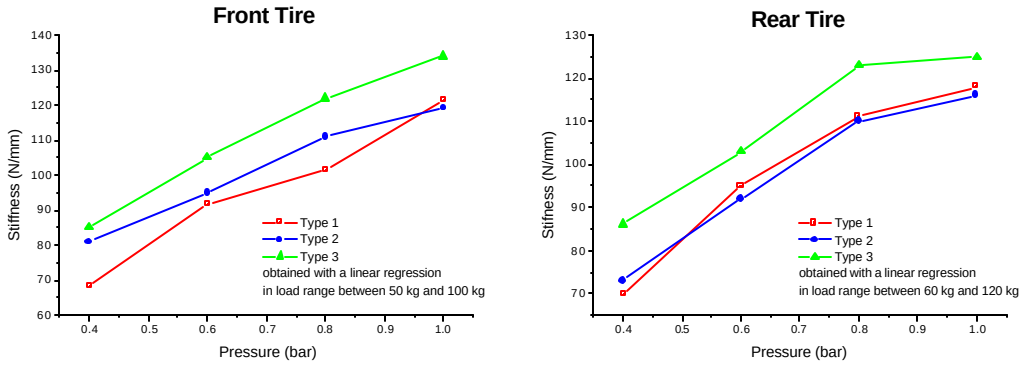

Figure 12: Radial stiffness of the tested tires for variable inflating pressures.

Static loading test

In order to check the reliability of the developed FEM model, an experimental test was carried out on the actual frame. The frame was clamped at the rear end and pinned on the front side. A vertical load was applied in the stub axle mounting point, one time on the right side and one time on the left side. This configuration is suitable to estimate the torsional behaviour of the frame. Displacement at points labelled “dx” and “sx” was recorded by a micrometer and load was applied by means of known weight. On a pre-load of 10 kg were applied more 10 kg and then another 10 kg; in the same way the frame was unloaded in step of 10 kg.

The experimental layout is illustrated in figure 13 together with the FEM model constraint scheme adopted, in which each constraint point suppress vertical translation, excepting two nodes constrained in order to avoid lability in horizontal plane.

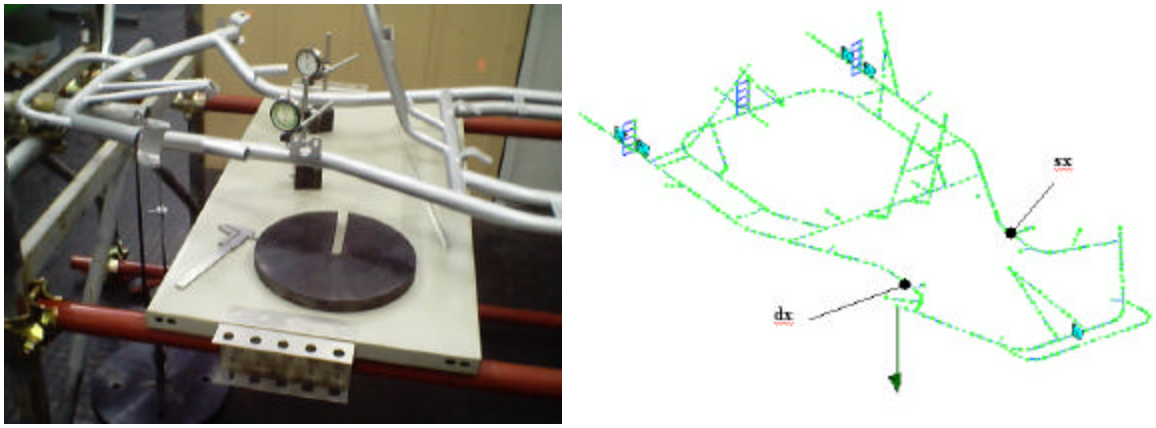

Figure 13: Static load testing: experimental layout; FEM model constraints and loads.

The experimental results are reported in the table. C1 indicate that the load is on the left side and C2 otherwise. The main discrepancies between numerical and experimental results are in the asymmetry observed experimentally and in the displacement in the point opposite to the loaded side. In our opinion the asymmetry is connected with lack of precision of the fixturing system and the manufacturing tolerances of the frame. Changing the side produces a different adjustment in the clearance recovery between fixtures and frame; furthermore the micrometer on the unload side is near its tolerance limit, thus its measure is not to be considered very accurate. Anyway, the excellent agreement on the loaded side confirms that the FEM model is representative enough of the actual frame.

	Total displacement (mm)				**Incremental displacement (mm)**			
Load (kg)	C1 (dx)	C1 (sx)	C2 (dx)	C2 (sx)	C1 (dx)	C1 (sx)	C2 (dx)	C2 (sx)
10	2.01	9.02	8.77	2.05				
20	2.08	9.62	9.35	2.09	0.07	0.6	0.58	0.04
30	2.15	10.26	9.95	2.16	0.07	0.64	0.6	0.07
20	2.09	9.66	9.37	2.11	-0.06	-0.6	-0.58	-0.05
10	2.02	9.06	8.78	2.04	-0.07	-0.6	-0.59	-0.07
					Incremental mean (mm)			
				Results →	0.0675	0.61	0.5875	0.0575
					Incremental FEM (mm)			
					0.1070	0.5904	0.5905	0.1071
					Error (%)			
					36	3.2	0.5	46

Table 2: Static test: experimental and numerical results.

The constraint condition is chosen to exclude bending effects being the vertical displacement at frame center suppressed by the vertical support, and is therefore suitable to estimate the torsional stiffness as:

$$M_T = Fb$$

$$\Delta y = b\Delta q \qquad (14)$$

$$K_T = \frac{M_T}{\Delta q} = \frac{Fb^2}{\Delta y}$$

Computed value (*b=314mm*) is 285000 N mm / deg and is consistent with literature values typical of a competition go - Kart (169000 in [6], 166000 in [9]).

Dynamic loading test

The second experimental check conducted regards the capability of the FEM model to represent the dynamic response of the frame.

As mentioned in the introduction, dynamic effects of the frame were neglected in the handling simulation, considering a quasi-static approach to evaluate load distribution, however the modal behaviour of the frame was investigated both to check the correctness of the discrete model and to prepare an input for further investigation.

Experimental analysis was conducted assuming a free-free constraint condition. This constraint was obtained experimentally hanging the frame in three points by means of soft rubber bands; the first six modes in this set -up have a very low frequency and are well distinguished from the natural ones.

The measurement layout consists in a load cell hammer, an accelerometer (both by "Kistler"), a signal amplifier, a data acquisition card and the analysis software DATS (figure 14).

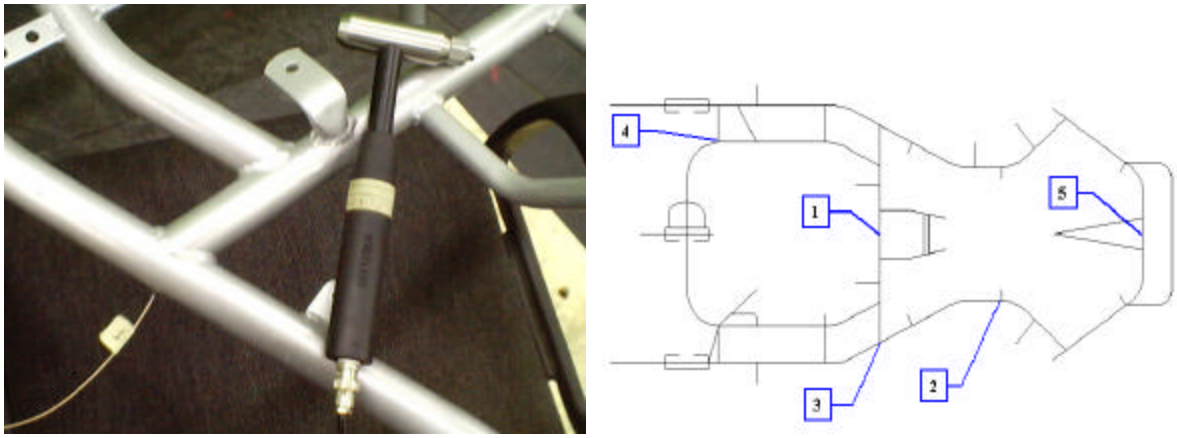

Figure 14: Dynamic load testing: experimental layout; excited and measured points.

Five points were considered, as depicted in figure 14. The response was recorded in 1 and 2 for impulsive excitation in each of the five points to give ten harmonic responses. Cross responses, illustrated in fig 15, were checked with an acceptable agreement for higher acceleration values but with poor amplitude reproduction at lower acceleration; however the peaks pattern agree very well.

To check the numerical model, first a modal analysis was performed, extracting 37 eigenvalues in the range 1-350 Hz (excluding the first six rigid body modes) then an harmonic response analysis was conducted in the range 30-350 step 2.5Hz, using the modal approach (extracting modes in the range 1-1000Hz) and a damping value equal to 1% of critical. Only out of plane modes are excited in this study, the lower are bending at 41.8 Hz and twisting at 46.5Hz. Their interaction is well resolved in the experimental results, as shown in figures 15, in which the experimental harmonic response is plotted together with the numerical results. The second twisting mode at 102.2 Hz is evidenced in a3m3. Higher order bending modes at 150Hz and 162Hz are underestimated by FEM model, but are still identifiable in a1m5. However modes at 303 Hz and 308Hz are well recognised in a1m1.

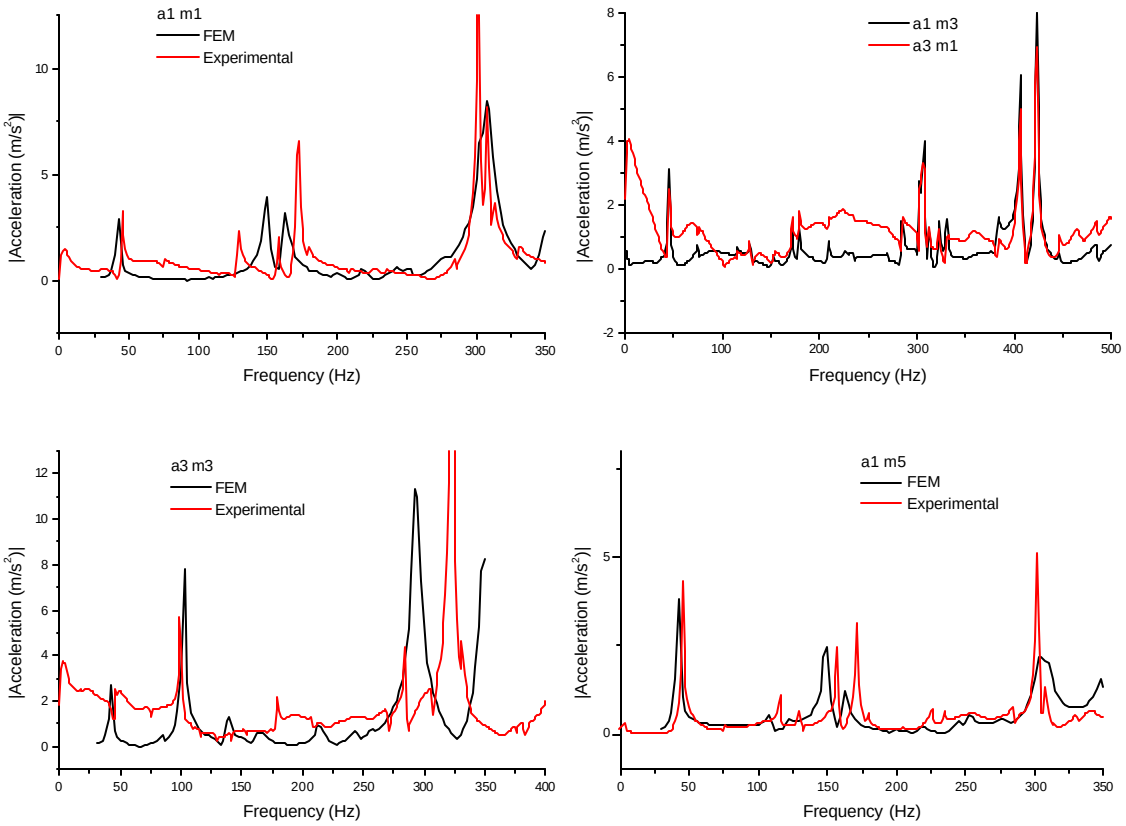

Figure 15: Harmonic response: experimental cross response 13 31; comparison between experimental and numerical responses 11 33 15.

RESULTS AND DISCUSSION

Handling model validation

To verify the correctness of the proposed handling model, a simulation test was conducted both on the proposed model and on a model, previously presented by the authors, developed for the commercial multibody software Working Model 3D 5.0.

The test consists in a sinusoidal input of the steering angle, with period 1 second and amplitude 5 degrees, imposing a constant value of longitudinal speed (15 m/s) achieved by a proportional control law.

Multibody model is depicted in figure 16 and is detailed described in [4,6].

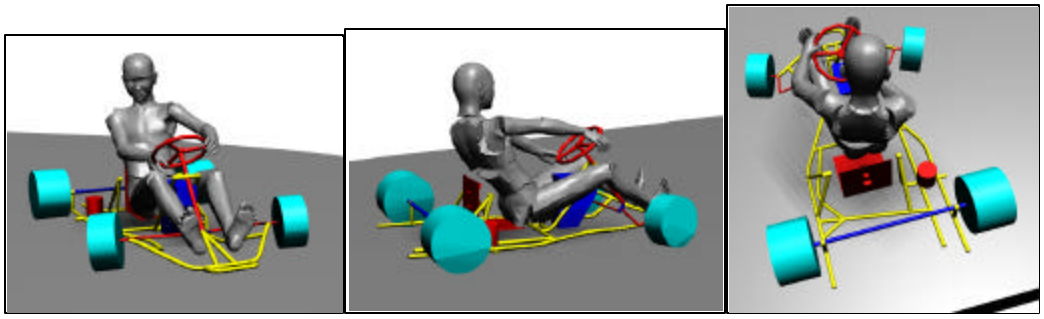

Figure 16: Multi-body model used for handling model validation.

Comparison was conducted assuming the same values for mass, tires and geometry (summarised in tab 1) and the same input; the compared output are the lateral acceleration and the yaw rate, as shown in fig 17.

Wheel base (a+b)	1.095 m (0.625+0.47)
Front track width (c_a)	0.96 m
Rear track width (c_p)	1.16 m
Centre of mass height (z_G)	0.246
Mass	135 kg
Yaw moment of inertia	11.0 kgm^2

Table 1: Parameters of the analyzed vehicle.

After a transient both model converge to the same solution; little differences are due probably to the effects of rolling and pitching dynamic, that is resolved by the three dimensional multi-body model, but are neglected in the proposed model.

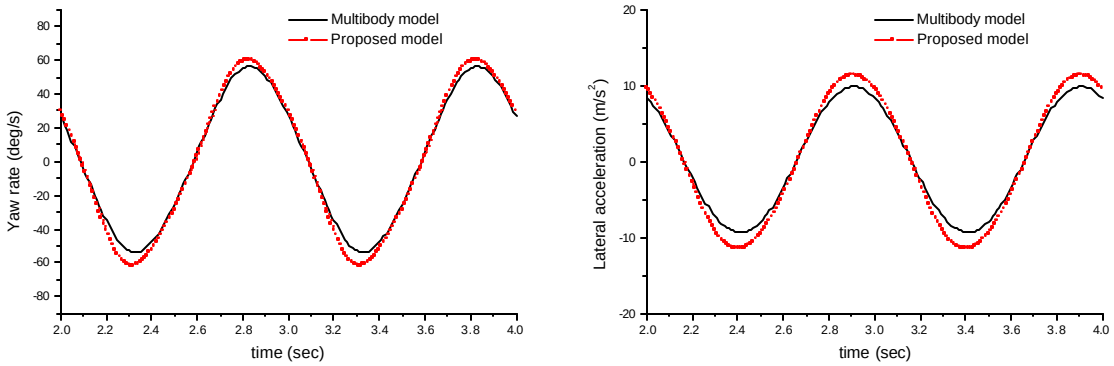

Figure 17: Yaw rate and lateral acceleration for the validation test, comparison between proposed model and literature model.

Road dynamic simulation

In order to investigate the influence of chassis geometry and its stiffness on dynamic vehicle behaviour, the model has been used to simulate the kart dynamic during a corner. The manoeuvre simulated is very similar to the one described in the introduction and includes the three typical phases (braking, cornering and acceleration). The input for the model is expressed by the time histories of steer angle and longitudinal speed shown in figure 18a. Being the steering angle an input for the simulation tool, it was simple processed in digital format; as far as the longitudinal speed is concerned, a proportional control law for an equivalent longitudinal force was imposed to follow the desired input.

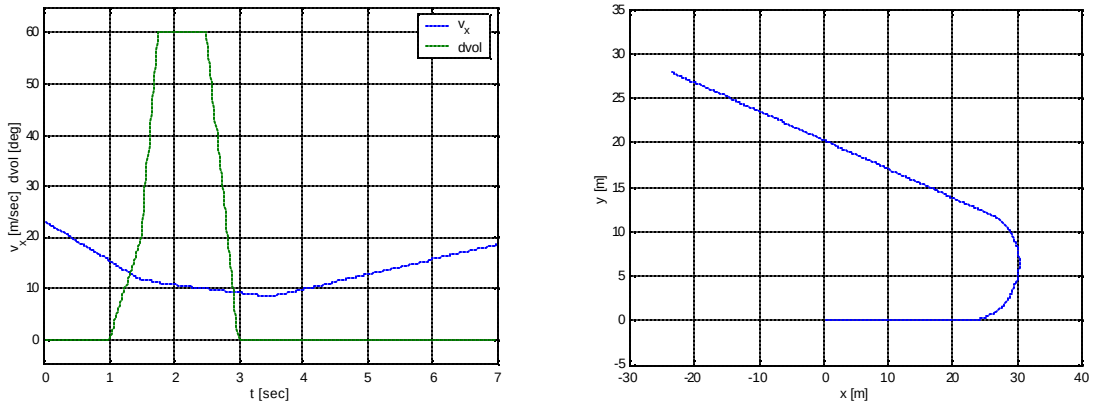

Figure 18: a) Prescribed steering angle and longitudinal speed vs time; b) Trajectory followed by the vehicle for the imposed inputs.

The trajectory for the original frame configuration is shown in figure18b. The same simulation was ran for four frame configurations: the first is the original configuration of the chassis; the second is derived by the first, removing the rear stiffening bar that is a set-up parameter. The third solution involve a redesign of the frame, replacing the original rear axle with a softer one, passing from a 45 mm diameter and 3 mm thickness to 35 mm diameter and 2 mm thickness. The fourth configuration was obtained considering a new diameter for the principal structure section, from a 30 mm diameter and 3 mm thickness to 28 mm diameter and 2 mm thickness.
A separate FEM model was developed for each configuration, extracting the stiffness matrix that was then inputted in the dynamic model.
Parametric analysis results are reported in the following figures, in which lateral acceleration (fig. 19) and vertical load on the rear internal tire (fig. 20), are plotted against elapsed time

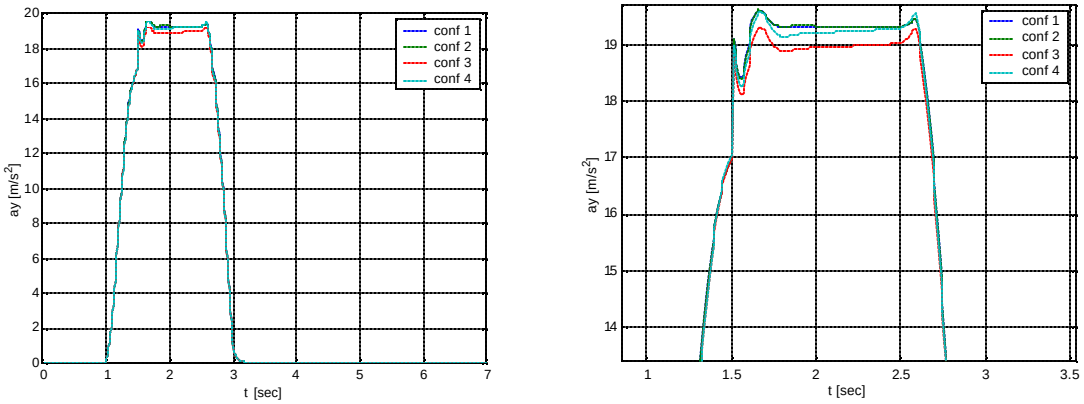

Figure 19: Full scale and detail of lateral acceleration for the analyzed solutions.

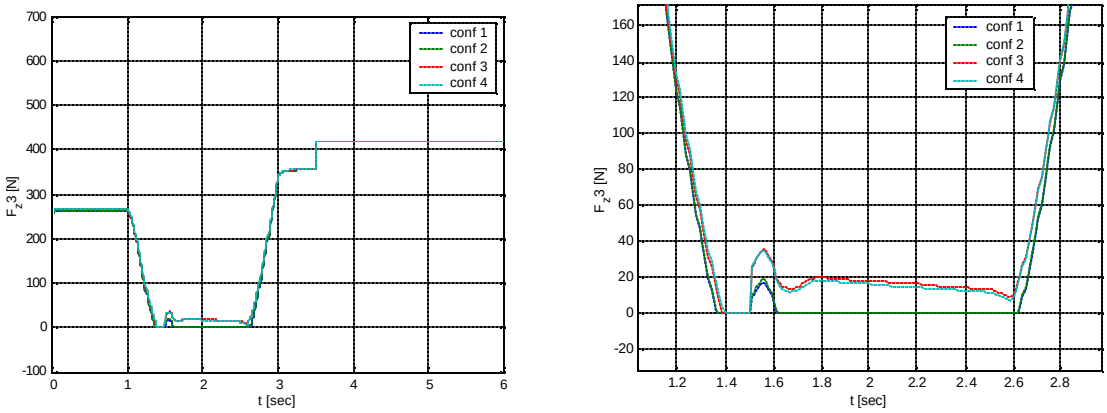

Figure 20: Full scale and detail of vertical loads for the analyzed solutions.

Is possible to notice that only configuration 1 and 2 (that are the stiffer ones) permit the rising of the rear internal tire. Observing acceleration diagram is possible to point out two results. First, configurations 1 and 2 allow to reach higher values of lateral acceleration; furthermore, in contrast to what was obviously foreseen, the lowest peak value doesn't correspond to the softer configuration (i.e. configuration 4), but instead is reached by configuration 3. This means that a reduction of single element stiffness doesn't necessarily involve a decrease of performance. Moreover one particular geometry solution can be suitable for a kind of track and very unfavourable for another circuit. Hence the influence of chassis stiffness must be studied into a very wide range of changes and it is very difficult to foresee the coupling of the effect of two different parameter variations . Thus an accurate structural optimisation can be successfully used to reach the ideal set-up in order to obtain the best performance in each condition.

CONCLUSIONS

In this paper the effects of frame compliance on vehicle behaviour was investigated. Interactions between the four wheels were evaluated by means of a FEM model and condensed in a compliance matrix. A vehicle dynamic model, able to manage FEM extracted compliance matrix, was developed.

A practical application of the model is presented for a competition go kart. This vehicle was chosen as representative to investigate the frame stiffness effects, because the lack of suspension system leaves the load transfer task to the frame and tires.

Several verifications were performed to check the reliability of the FEM model of the studied frame, including static and dynamic loading conditions; the results of such verifications show that the FEM model is reliable to represent the actual stiffness of the frame.

To properly consider load transfer, radial stiffness of the complete wheel, including tire, wheel-rim and bearing, was evaluated experimentally.

Lateral behaviour of the tire was modelled by a simple linear model using literature data.

Proposed model was first checked using as a reference a complete three dimensional model, proposed by the authors for a commercial multibody code, and then used for a parametric analysis of frame stiffness effects, considering several frame modifications.

To test the performance of four proposed frame solutions, a reference manoeuvre was chosen in which the vehicle, after a braking phase, approaches and travels a curve and then leaves it accelerating toward the straightaway. As mentioned in the introduction load transfer plays a crucial role because the rising of internal rear wheel is desired in order to compensate the lack of differential gear. Performed analyses show that the best results in terms of lateral acceleration developed during the prescribed manoeuvre, are obtained using the stiffer solution; however the worst solution is not the softer one, showing that a trend prediction is not applicable and that only a deep insight, achieved by the simulation tool, allows to compare properly analysed set-up.

Of course, presented parametric analysis is only a good starting points for the definition of a new design methodology in which the frame is optimised, in order to achieve the better race performance within the prescribed strength performance. Furthermore, the introduction of a shape optimisation [1] algorithm, seems feasible to converge in a semiautomatic way to an optimal solution in which structural parameters are varied to obtain a goal in dynamic simulation results, minimising, for instance, the lap time.

ACKNOWELDGMENTS

The authors would like to express their acknowledgements to Mr. Stefano Modena for his suggestions and for the furniture of tested tires, frame and tire fixturing device. The authors would like to thank Eng. Luciano Cantone for his help in dynamic measurement and dynamic data interpretation.

BIBLIOGRAPHY

[1] M. E. Biancolini, C. Brutti, E. Pezzuti, “Shape optimisation for structural design by means of Finite Elements Method”, ADM 2001, 12 th International Conference on Design Tools and methods in industrial engineering, Rimini, Settembre 2001

[2] Larry L. Howell, “ Compliant Mechanisms”, Ed. John Wily & Sons inc, 2001.

[3] “Eureka Brokerage Event Auto 2005 – Advanced Technologies for New Gheneration of vehicles” – Valencia, November, 25 - 26 1999

[4] E. Pezzuti, M. E. Biancolini, A. Ubertini, A. Gaspari, “CAD 3D Modeling of human body for movement analysis”, submitted for presentation at XIV Congreso Internacional de Ingeniería Gráfica, Santander, España 5-7 junio de 2002

[5] F. Barizzone, C. Campanile, L.Celiberti, A. Rosati, E. Pennestrì, P. P. Valentini, “ The development of a virtual dummy for the vibrational comfort analysis of car drivers”, VI U.S. National Congress on Computational, Dearbourne (MI), August 1-4 2000.

[6] R. Baudille, M. E. Biancolini, C. Brutti, L. Reccia, “Analisi integrata multibody FEM del comportamento dinamico di un kart”, AIAS 2001, XXX Convegno Nazionale dell'Associazione Italiana per l'Analisi delle Sollecitazioni, Alghero, Settembre 2001

[7] M. E. Biancolini, C. Brutti, L. Reccia, D. Del Pin "Three Dimensional Dynamic Model for a Quick Simulation of Vehicle Collisions", SAE Proceedings, ATTCE – Automotive and Transportation Technology Congress, Barcelona,1- 4 October 2001.

[8] B. Jang, D. Karnopp, "Simulation of vehicle and power steering dynamics using tire model parameters matched to whole vehicle experimental results", Vehicle System Dynamics, 33 (2000) pp 121-133.

[9] E. Guglielmino, I.D. Guglielmino, G. Mirone, “Caratterizzazione numerica e sperimentale di un Go-Kart da competizione” AIAS 2000, Lucca, settembre 2000.

[10] A. Di Benedetto, E. Pennestrì, “Introduzione alla cinematica dei meccanismi”, Ed. Ambrosiana, Milano.

[11] F. R. Williams, T. J. Dutek, “Load-deflection hysteresis and its relationship to tire rolling resistance” 122nd Rubber Division Meeting, American Chemical Society, Chicago, Illinois, Oct 5-7 1982.

[12] M. Giglio, A. Pecchio, P. Ravasi, “L’utilizzo del FEM per l’ottimizzazione di un telaio di Go-Kart” ATA Ingegneria Automobilistica, 2000.